Int. J. Heat Mass Transfer. Vol. 28, No. 10, pp. 1837–1846, 1985
Printed in Great Britain

0017-9310/85 $3.00 + 0.00

Measurements and calculations of transient mixed convection in air

BAHGAT SAMMAKIA,* V. P. CAREY† and B. GEBHART‡

*IBM Corporation, Dept. U51, Endicott, NY 13760, U.S.A.;
† Department of Mechanical Engineering, University of California, Berkeley, CA 94720, U.S.A.;
‡ Department MEAM; University of Pennsylvania, Philadelphia, PA 19104, U.S.A.

(*Received* 19 *March* 1984 *and in final form* 26 *March* 1985)

Abstract—Measurements and calculations of transient mixed convection flows adjacent to a flat vertical surface are presented. The surface dissipates a constant and uniform heat flux in an air stream flowing at a uniform and constant ambient velocity. The free-stream velocity is in the same direction as the buoyancy-induced flow resulting in an 'aiding' mixed convection flow. Temperature and velocity measurements in the boundary layer are presented and compared to the results of a finite-difference analysis of the flow. Several heat flux levels and ambient stream velocities are investigated.

INTRODUCTION

INTEREST in mixed convection flow is motivated by the many technological, as well as environmental circumstances under which such flows may arise. Most previous studies, however, have considered steady-state circumstances. Such studies include those by Sparrow and Gregg [1], Lloyd and Sparrow [2], Oosthuizan and Hart [3], Gryzagoridis [4], and Hommel [5].

Merkin [6] investigated both aiding and opposing flows adjacent to a flat vertical isothermal surface. The solution was obtained by using expansions near the leading edge and far downstream, then closing the gap between the two solutions with a numerical marching scheme. Wilks [7] applied a similar technique to a surface dissipating a uniform and constant heat flux. For aiding flows, forced convection effects were found to dominate near the leading edge, while far downstream, the flow takes on natural convection characteristics.

Carey and Gebhart [8] presented a perturbation analysis of the mixed convection flow adjacent to a vertical uniform flux surface which included both higher-order boundary layer and mixed convection effects. Measurements of steady-state aiding flows in air were found to be in good agreement with the analytical results. Hunt and Wilks [9] compared the measurements in [8] to the theory in [7] and reported that while the numerical solution of the boundary-layer equations is adequate in the vicinity of the surface, higher-order effects are significant at large distances from the surface.

Despite their importance in many applications, transient mixed convection flows have received much less attention than the steady flows mentioned above. Sammakia *et al.* [10] presented a finite-difference analysis of the transient, aiding, mixed convection flow. Results for both uniform heat flux and isothermal boundary conditions were presented with $Pr = 0.72$ and 7.6. For the uniform flux circumstance, the steady-state results compared favorably with those of the perturbation analysis presented by Carey and Gebhart in [8].

Although the calculated results of Sammakia *et al.* [10] are based on a sound theoretical foundation, such calculations have not been verified experimentally. In fact, we are aware of no previous experimental studies of transient mixed convection flow near a vertical surface. In the present study, new measurements of temperature and velocity profiles have been obtained for laminar transient mixed convection near a vertical uniform-heat-flux surface. Measured profiles at a single downstream location are reported for several combinations of free-stream velocity and heat flux. These measurements are then compared to the results of a numerical analysis similar to that in [10].

EXPERIMENTAL

Figure 1 shows the experimental set-up used to measure transient temperature and velocity profiles. The cylindrical test section had an inner diameter of 33.7 cm and was 76.2-cm high. To achieve a uniform flux surface, an inconel 600 foil, 15-cm wide and 0.0127-cm thick, was heated by passing an electric current through it. The foil was held in place by stretching it on a special support fixture. Near the leading edge the foil was looped around a tape-covered aluminum support, while at the trailing edge it was held by a spring loaded knife-edge. This spring loading exerted an upward stretching force on the foil ensuring its uniformity during the heating process. The gap formed by the two sides of the foil was filled with foam insulation of 0.635-cm thickness. The resulting surface was 15-cm wide, 40-cm long, and 0.637-cm thick. The surface was aligned vertically with a horizontal leading edge by using a plumb line and level.

The surface was heated by passing an electrical current through it. This was accomplished by using a

NOMENCLATURE

c'' thermal capacity of element per unit surface area
g acceleration of gravity
Gr_x Grashof number $(g\beta\Delta Tx^3/\nu^2)$, dimensionless
Gr_x^* modified Grashof number $(g\beta q''x^4/k\nu^2)$, dimensionless
k thermal conductivity
L height of plate
Pr Prandtl number
q'' instantaneous energy generation rate per unit of element surface area
Q^* thermal capacity parameter related to the element storage capacity $c''(g\beta q''\nu^2/k^5)^{1/4}$
t static temperature
t_0 instantaneous local plate temperature
t temperature of the undisturbed fluid
u component of velocity in vertical direction
v component of velocity in horizontal direction
x vertical distance above bottom of plate
y horizontal distance from plate.

Greek symbols
ν kinematic viscosity
ρ density of fluid
τ time
τ non-dimensional time, =TAU.

Subscripts
0 at solid–fluid surface
∞ free-stream conditions
T total input
R radiation
C convective
avg average.

regulated power supply. The voltage drop across the foil was measured by using a Hewlett Packard 3465B digital multimeter. To measure the current in the circuit, the voltage drop was also measured across a Leeds and Northrup 0.01 Ω, 100 A standard shunt, connected in series to the foil. Knowing the voltage drop across the foil, and the current passing through it, the dissipated heat flux could be computed.

Air was supplied to the test section from a compressed air storage tank maintained at about 7 atm pressure. Air from the storage tank was passed through a pressure regulator, and critical orifice meter, before entering the test section. The air pressure in the storage tank was maintained by compressors operating in a cycling fashion. To maintain a uniform free-stream velocity in the test section it was necessary to maintain critical flow conditions at the orifice meter. The flow through the test sections was thus a function of the pressure upstream of the meter which was held to within ± 0.07 atm (± 7 kPa) by the pressure regulator. Temperature fluctuations in the air supply were measured and found to be less than 0.05°C during any test. This system had a peak flow capacity of about 0.7 $m^3\ s^{-1}$ at atmospheric pressure, resulting in a peak mean velocity of 7.5 $cm\ s^{-1}$ in the test section.

To ensure uniform flow distribution over the test section, flow baffles were placed at the bottom and top of the test section. Flow uniformity was confirmed by

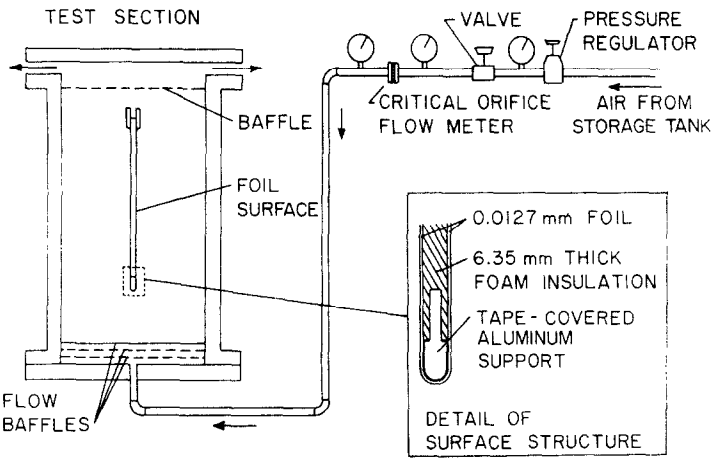

FIG. 1. Schematic diagram of experimental set-up used to measure transient temperature and velocity profiles in aiding mixed convection flow.

taking hot film measurements across the test section which indicated a maximum variation of ± 0.1 cm s^{-1}. During the experiments the variation of the core velocity with vertical location was found to be small. The flow acceleration in the core region due to entering a cylindrical section was, to some extent, negated by the flow acceleration due to buoyancy near the heated surface. The support structure for the surface was designed to minimize drag and the structural members were distant from the heated surface.

The primary objective of the experiment was to take velocity and temperature measurements, during the transient, at several boundary-layer locations. Velocity was measured using a Disa 55M01 constant-temperature hot wire anemometer with a Disa 55P14 miniature probe. The output was recorded on a Hewlett Packard model 5150A thermal printer. The hot-wire probe was L-shaped to minimize probe interference with the flow. The probe was calibrated in air at an overheat ratio of 1.6, for velocities up to 40 cm s^{-1}. The hot-wire output was corrected, to account for varying ambient temperature, using the procedure outlined by Mahajan [11]. A detailed discussion of the calibration procedure may be found in Carey [12].

Temperatures were measured using a 0.0254-mm copper–constantan thermocouple. To minimize conduction loss in the leads, the two leads were horizontal and parallel to the surface, thereby lying along an isotherm. The leads were then passed through a pair of 1.0-mm hollow glass tubes attached to a support situated outside the boundary layer. The ambient air temperature in the tank was measured using a 0.0127-cm copper–constantan thermocouple. An ice bath was used as a reference for both thermocouple junctions. The temperatures were measured using a Hewlett Packard 3465B multimeter and recorded on a Hewlett Packard 5150A thermal printer.

Both the temperature and velocity boundary-layer probes were connected to a single support mounted on a traversing mechanism. A 1.5-mm copper rod was also attached to the same support and used to locate the foil. This was accomplished by passing an electric current through the rod and monitoring the resistance of that circuit. As the rod contacted the foil the circuit was completed and the resistance drops to some small value. The velocity, temperature, and surface probe were always in the same horizontal plane. The relative positions of the thermocouple junction, the hot-wire sensor, and the surface probe were determined from an enlarged photograph of the assembly.

The probe array was located at a downstream location 31.4 cm from the leading edge and all measurements were taken there. To traverse the boundary layer the probe array was mounted on a Disa 55H01 traversing mechanism. This was driven by a Disa 52C01 stepper motor which was remotely controlled by a Disa 52B01 sweep drive unit. The probe could thus be accurately moved in steps of 0.203 mm and displayed on the mechanical counter of the sweep drive unit.

Velocity and temperature measurements were taken at the combinations of heat flux and free stream velocities shown in Table 1. Basically, four different cases were studied. Cases 1 and 2 constitute high Gr_x^* flows (order of 10^9) with $Re_x = 622.3$ and 831.2, respectively. Whereas, for cases 3 and 4, Gr_x^* is lower (order of 10^8) with $Re_x = 748.1$ and 1081.1, respectively. These parameters ensure covering a wide range of relative significance of forced convection effects. These effects are strongest for case 4, followed by cases 3, 2 and 1, respectively. A transient test was run three or four times for each case listed in Table 1, with the traversing probe in a different y location for each run. From the temperature and velocity histories thus determined at each location, the variation of the velocity and temperature profiles with time could be inferred. Transient tests were done at four locations for cases 1 and 3 (A, B, C and D), and three locations for cases 2 and 4 (A, B and C), as shown in Table 1.

Due to slight variations in ambient conditions and upstream pressure levels in the storage tank, it was not possible to exactly duplicate the free-stream velocity and heat flux levels. Average values were computed for each case and used in the subsequent numerical computations. The maximum difference between any heat flux level and the average value used is about 2.5%, while for the free-stream velocity it is about 5%. To determine the convective heat flux, q_C'' from the electrical input, it was necessary to compute the heat flux emitted by radiation from the surface. The procedure outlined in [12] was followed, and the q_R'' values are shown in Table 1.

NUMERICAL SCHEME AND RESULTS

Equations (1)–(3) are the non-dimensional equations of motion representing conservation of mass, momentum, and energy, for a mixed convection flow adjacent to a flat vertical semi-infinite surface. The equations embody both the boundary-layer and Boussinesq approximations

$$\frac{\partial U}{\partial X} + \frac{\partial V}{\partial Y} = 0 \tag{1}$$

$$\frac{\partial U}{\partial \tau} + U\frac{\partial U}{\partial X} + V\frac{\partial U}{\partial Y} = T + \frac{\partial^2 U}{\partial Y^2} \tag{2}$$

$$\frac{\partial T}{\partial \tau} + U\frac{\partial T}{\partial X} + V\frac{\partial T}{\partial Y} = \frac{1}{Pr}\frac{\partial^2 T}{\partial Y^2}. \tag{3}$$

For a uniform heat input boundary condition, the non-dimensionalization and boundary conditions for $\tau > 0$ are

$$T = \frac{t - t_\infty}{(\nu^2 q''^3/g\beta k^3)^{1/4}} = \frac{t - t_\infty}{q'' x/k}(Gr_x^*)^{1/4},$$

$$\tau = \frac{\bar{\tau}}{(k/g\beta q'')^{1/2}} = \frac{\alpha\bar{\tau}}{x^2} Pr(Gr_x^*)^{1/2} \tag{4a}$$

Table 1. The values of surface heat flux levels, free-stream velocities, locations at which measurements were taken, and some of the relevant non-dimensional parameters

Run		t_∞ (°C)	u_∞ (cm s^{-1})	u_{ave_g} (cm s^{-1})	y (cm)	q''_T (W m^{-2})	q''_R (W m^{-2})	q''_C (W m^{-2})	q''_{ave_g} (W m^{-2})	Gr^*_x ($\times 10^{-8}$)	X	Y	Q^*	Re_{x_∞}	U_∞	U_{max}/U_∞
1	A	20.3	2.9	3.0	0.295	51.45	13.75	37.7	37.3	21.2	214.6	1.98	40.6	622.3	2.9	6
	B	20.3	3.1		0.497	50.19	13.75	36.44				3.35				
	C	20.4	3.2		0.803	51.23	13.59	37.64				5.4				
	D	20.3	3.0		1.110	51.29	13.85	37.44				7.45				
2	A	19.5	4.3	4.0	0.295	50.85	12.62	38.23	36.74	20.8	213.7	1.97	40.5	831.2	3.89	4.5
	B	19.5	4.0		0.6	49.55	12.99	36.56				4.01				
	C	19.5	3.8		0.904	49.27	13.82	35.45				6.06				
3	A	19.2	3.8	3.6	0.345	14.95	4.01	10.94	10.74	6.16	157.5	1.7	29.8	748.1	4.75	3.1
	B	19.2	3.6		0.6	14.79	4.29	10.5				2.96				
	C	19.2	3.6		0.802	15.08	4.51	10.57				3.96				
	D	19.2	3.6		1.00	15.23	4.29	10.94				4.96				
4	A	19.3	5.4	5.1	0.345	14.19	3.82	10.37	10.44	5.93	156	1.69	29.5	1081.1	6.93	2.17
	B	19.3	5.0		0.6	14.19	3.75	10.44				2.93				
	C	19.3	5.0		1.25	14.45	3.94	10.51				4.18				

$$U = \frac{u}{(v^2 g\beta q''/k)^{1/4}} = \frac{ux/v}{(Gr^*_x)^{1/4}},$$

$$U_\infty = \frac{u_\infty x/v}{(Gr^*_x)^{1/4}} = \frac{u_\infty}{(v^2 g\beta q''/k)^{1/4}} \tag{4b}$$

$$V = \frac{v}{(v^2 g\beta q''/k)^{1/4}} = \frac{vx/v}{(Gr^*_x)^{1/4}} \tag{4c}$$

$$X = \frac{x}{(v^2 k/g\beta q'')^{1/4}} = (Gr^*_x)^{1/4},$$

$$Y = \frac{y}{(v^2 k/g\beta q'')^{1/4}} = \frac{y}{x}(Gr^*_x)^{1/4} \tag{4d}$$

$$Y = 0, \quad U = V = 0 \tag{4e}$$

$$Y = 0, \quad 1 = Q^*\left(\frac{\partial T}{\partial \tau}\right) - \left(\frac{\partial T}{\partial Y}\right) \tag{4f}$$

$$Y \to \infty, \quad T \to 0, \quad U \to \frac{u_\infty x/v}{(Gr^*_x)^{1/4}} = \frac{Re_x}{(Gr^*_x)^{1/4}} = U_\infty \tag{4g}$$

$$X = 0, \quad U = U_\infty. \tag{4h}$$

Equation (4f) is an energy balance at the solid–fluid interface. The first term on the RHS is the changing heat storage in the surface element. The second term is the energy convected by the fluid. Q^* is given by

$$Q^* = c''\left[\frac{v^2 g\beta q''}{k^5}\right]^{1/4} = \frac{c''}{\rho c_p x} Pr(Gr^*_x)^{1/4}. \tag{5}$$

The initial conditions were $T = 0$ for the temperature field, and the Blasius flow velocities for the established velocity field. The latter were determined by solving equations (1) and (2) with $T = 0$ in (2), and subject to conditions (4g) and (4h). In an explicit finite-difference scheme the solution marched forward in time till the steady-state Blasius flow velocities were reached. This velocity field was then used as an initial condition for the mixed convection problem.

The numerical scheme used for calculating the mixed convection problem was also an explicit finite-difference scheme. The solution started at $\tau = 0$, at which time the heat flux into the surface is assumed to commence. At every time step the changing temperature and velocity fields were computed. The solution was marched forward in time until a steady state was reached at which time the temperature and velocity fields remain constant. The relevant parameters in the numerical calculations are X, U_∞ and Q^*. These were determined according to the specific run and are shown in Table 1. The numerical scheme is detailed in refs. [10] and [13]. In [10] the resulting steady-state temperature and velocity distributions are compared to the results of the perturbation analysis from [8], with good agreement.

Figure 2 shows five transient temperature response profiles for run 1 in Table 1. Numerical results are shown as solid circles, and the measurements as solid symbols. The results are plotted in terms of the non-dimensional variables T and Y, at five values of the non-

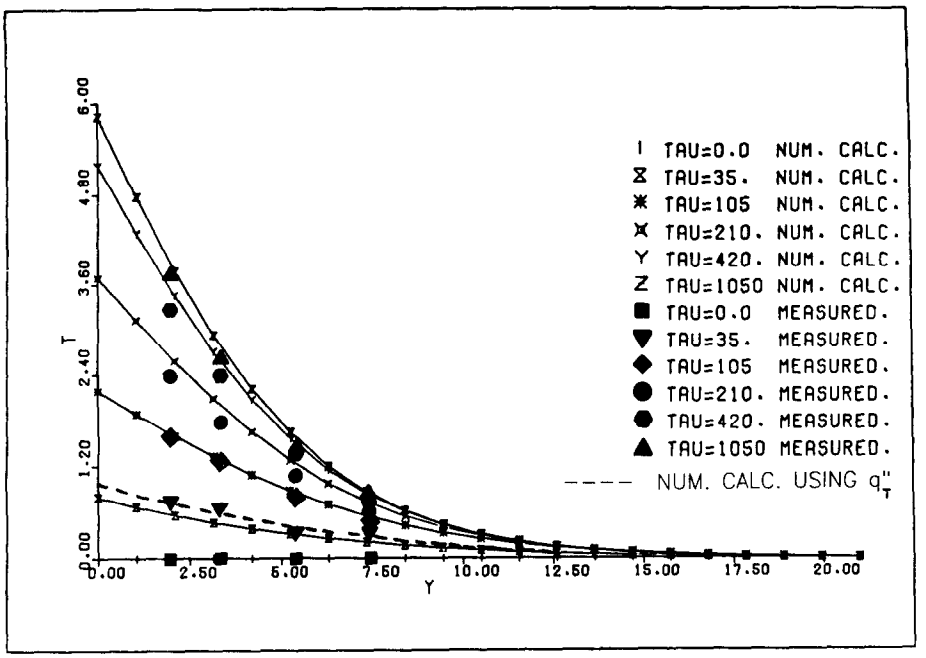

FIG. 2. Transient temperature profiles for run 1 in Table 1. Solid lines are computed profiles, solid symbols are boundary-layer measurements.

dimensional time TAU = τ. This case corresponds to $Gr_x^* = 21.2 \times 10^8$, $Re_x = 622.3$. This combination of parameters leads to a steady state dominated by natural convection effects. The total transient time for this case was about 150 s. At early times, $\tau = 35$, the measured temperatures exceed the computed values by about 20%. At later times the computed results show better agreement with the measurements, with a maximum difference of 10%, $\tau = 210$, and about 4% at $\tau = 1050$.

The large differences at early times is at least partly due to adjusting the heat flux used in the calculations to account for radiation. The convective heat flux, q_C'', is about 23% lower than the actual heat flux input to the surface, q_T''. The difference between the two values, q_R'', is emitted by the surface to the surroundings by thermal radiation. This value of q_R'' is based on steady-state measurements. During the early transient, the surface temperature is considerably closer to that of its surroundings and q_R'' is correspondingly lower than that at steady state. Thus at short times the heat flux used in the calculations, q_C'', is actually lower than that convected by the fluid adjacent to the surface in the experiment. As a check of the effect of the radiation heat flux correction on the early transient solution, run 1 was re-calculated using q_T'' in the numerical procedure. The results shown for $\tau = 35$ in Fig. 2 show much better agreement with the measured temperature response.

The temperature field is seen to increase monotonically with time. That is there were no local overshoots anywhere in the flow field. This was found for all the circumstances investigated in the present study.

Figure 3 shows the velocity response for run 1. Again, as for the temperature profiles, the measured velocities exceed the computed values during the early transient. This is expected however, since the velocity field is largely driven by the buoyancy force, generated from the temperature field. The agreement is quite good and improves with increasing time. A small overshoot occurs locally, in the computed velocity profiles, during the transient. These overshoots away from the surface are possibly due to the development of increased entrainment, the v component of velocity, as steady state is approached.

An interesting feature of this transient aiding flow is that the Y location at which the maximum velocity occurs shifts inward toward the surface with time. This is seen in Fig. 3, where the maximum velocity occurs at around $Y = 3.8$ at $\tau = 105$, and eventually moves to $Y = 2.9$ at $\tau = 1050$. This shift follows from the development of the buoyancy-induced velocity field with increasing time.

Figures 4 and 5 are, respectively, the transient temperature and velocity profiles for run number 2 in Table 1. Here the ratio $Re_x/(Gr_x^*)^{1/4} = U_\infty$ is 3.89, slightly higher than for run number 1. Agreement between measurements and calculations, and other features of the transient regime are similar to those observed in run number 1. In steady state, the ratio of U_{max}, the maximum velocity in the boundary layer, to U_∞ is about 4.5. This indicates that buoyancy effects are, as in run number 1, relatively dominant in steady state. Here also the Y location of U_{max} shifts with time as buoyancy develops.

For run number 3 in Table 1, $U_\infty = 4.75$, and the ratio $U_{max}/U_\infty = 3.15$. Figures 6 and 7 show, respectively, the transient temperature and velocity

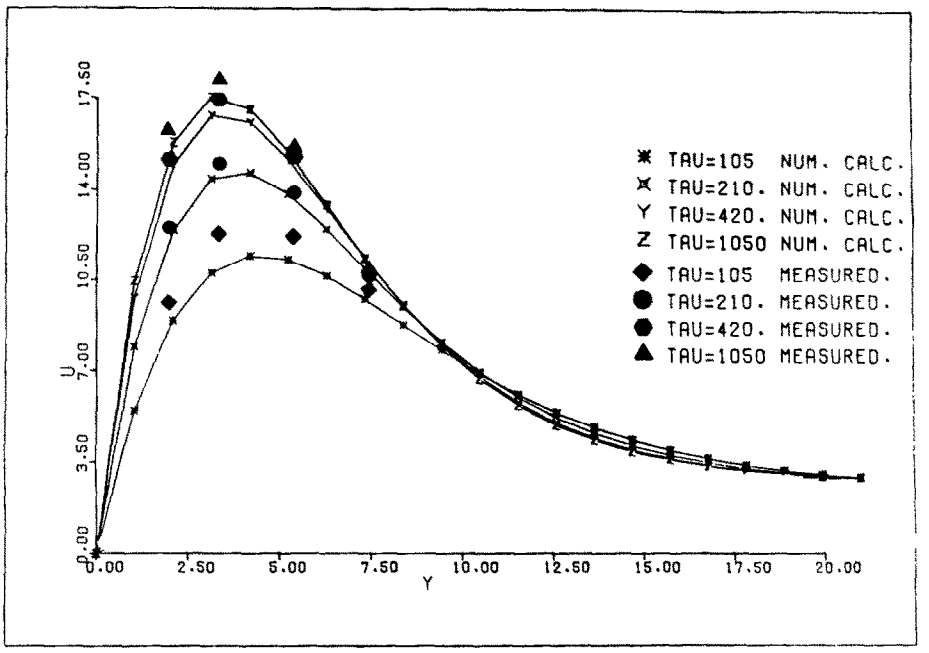

FIG. 3. Transient velocity profiles for run 1 in Table 1. Solid lines are computed profiles, solid symbols are boundary-layer measurements.

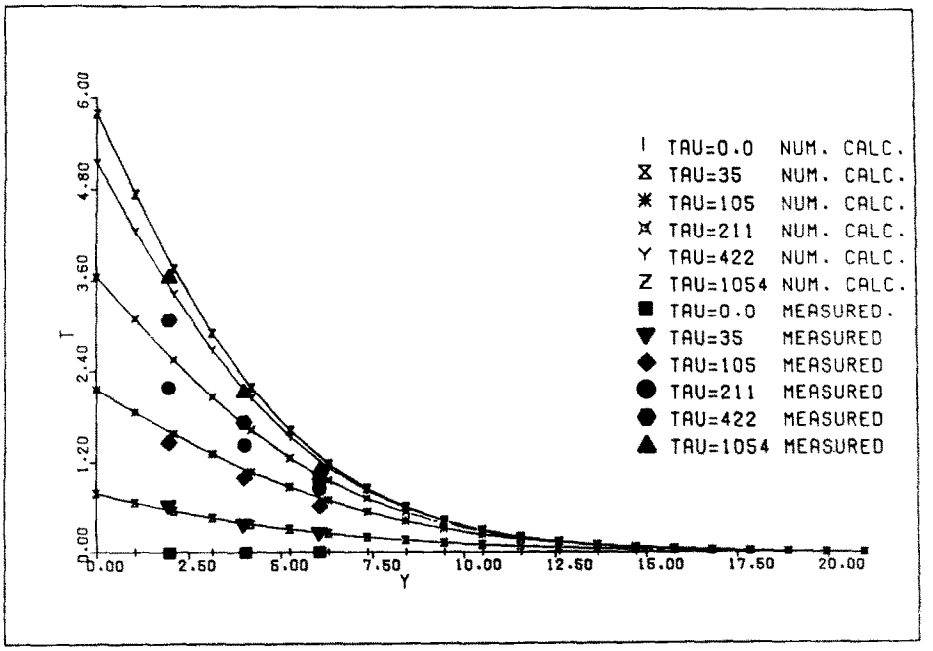

FIG. 4. Transient temperature profiles for run 2 in Table 1. Solid lines are computed profiles, solid symbols are boundary-layer measurements.

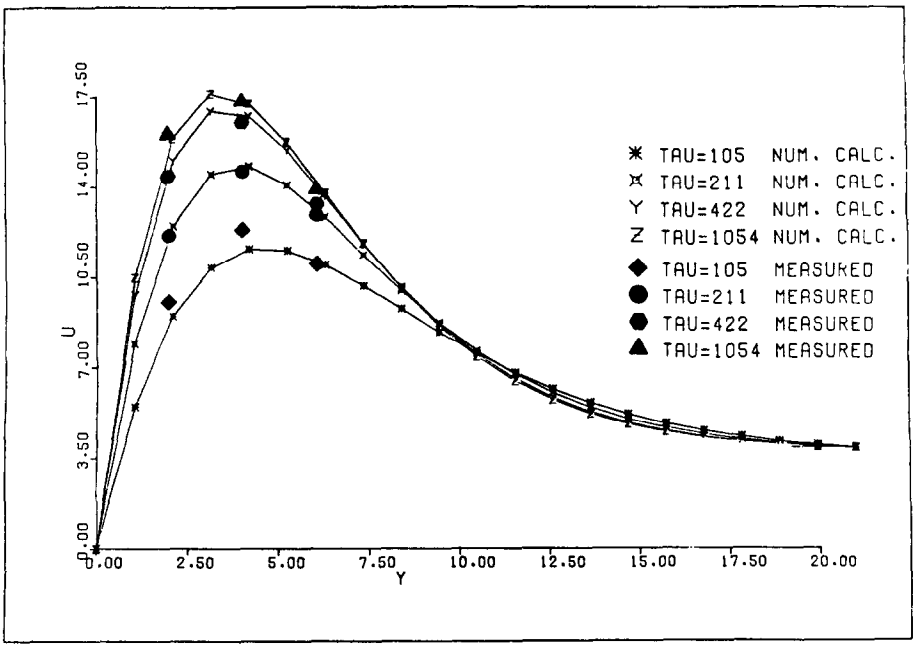

FIG. 5. Transient velocity profiles for run 2 in Table 1. Solid lines are computed profiles, solid symbols are boundary-layer measurements.

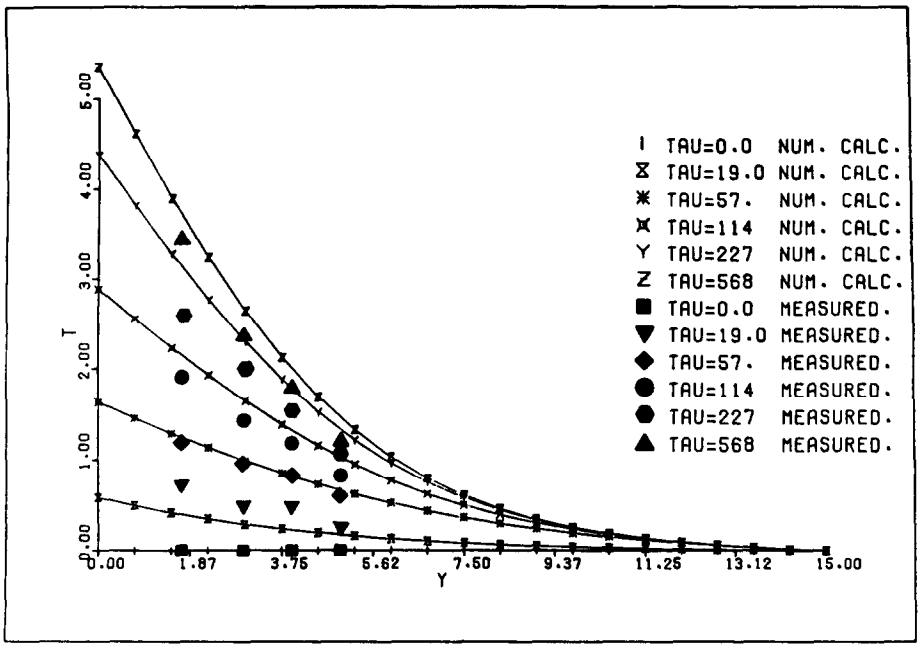

FIG. 6. Transient temperature profiles for run 3 in Table 1. Solid lines are computed profiles, solid symbols are boundary-layer measurements.

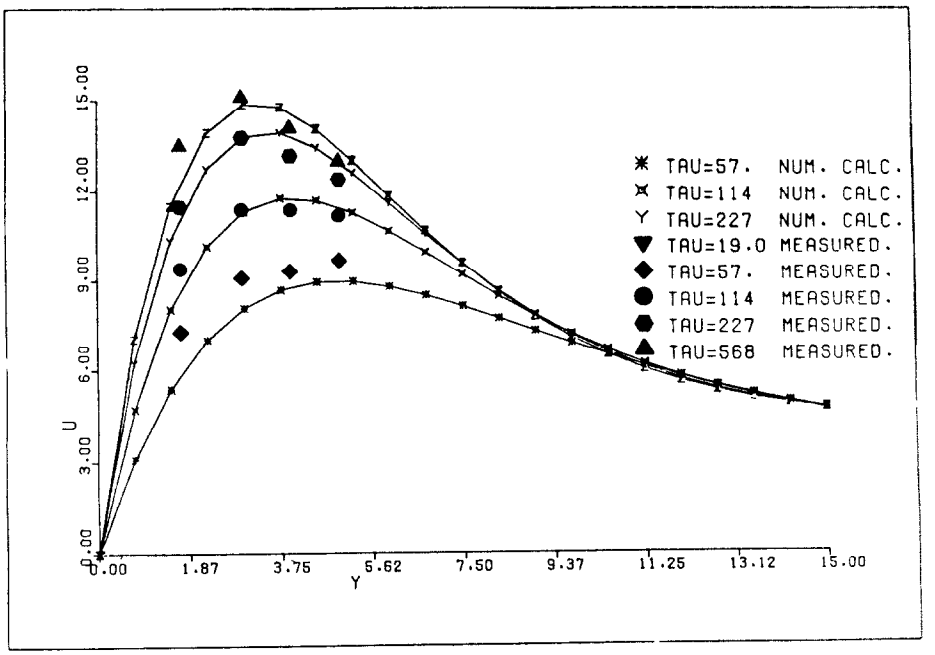

FIG. 7. Transient velocity profiles for run 3 in Table 1. Solid lines are computed profiles, solid symbols are boundary-layer measurements.

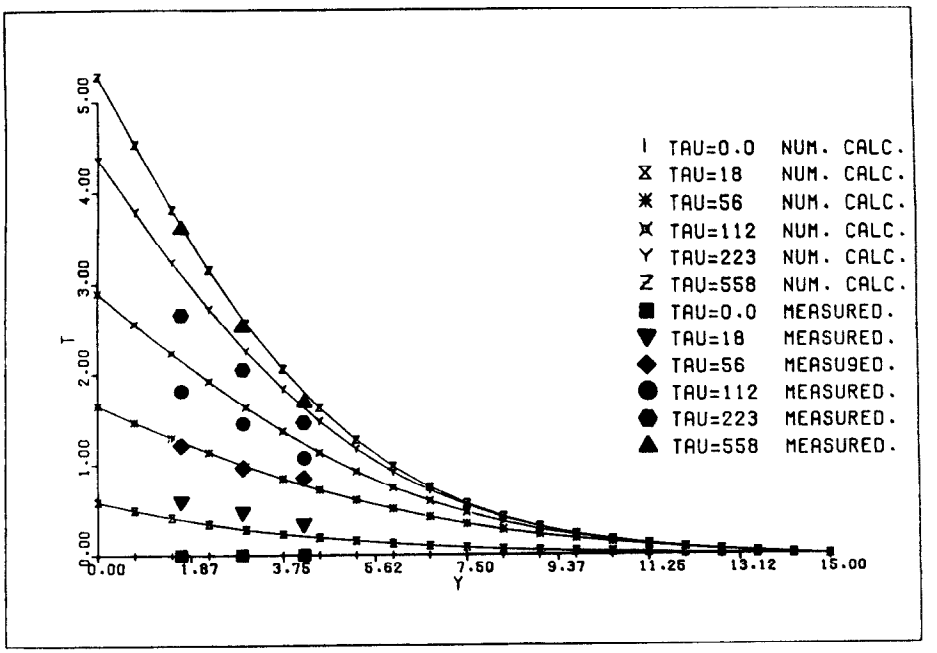

FIG. 8. Transient temperature profiles for run 4 in Table 1. Solid lines are computed profiles, solid symbols are boundary-layer measurements.

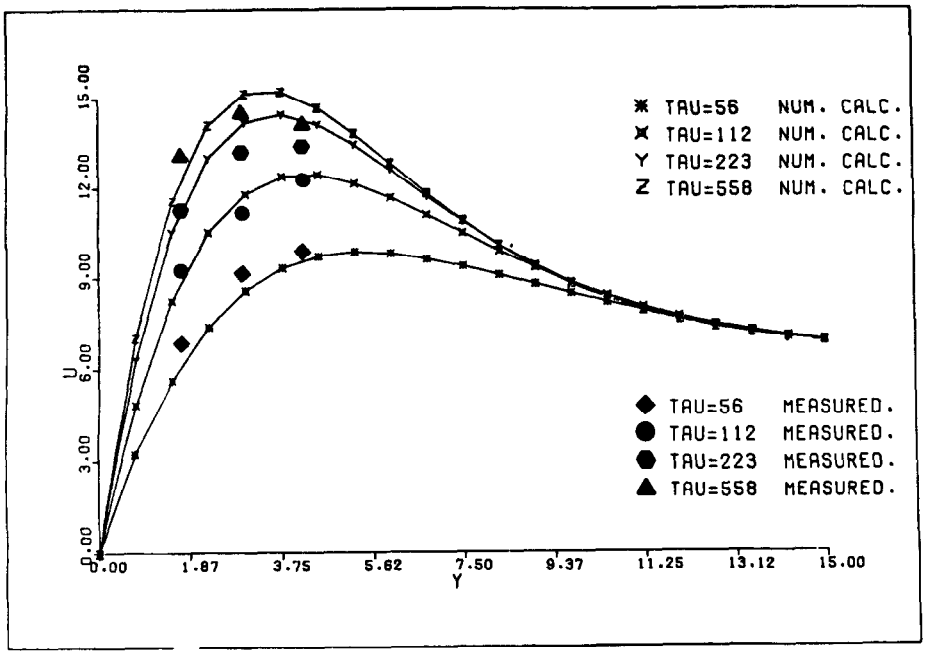

FIG. 9. Transient velocity profiles for run in Table 1. Solid lines are computed profiles, solid symbols are boundary-layer measurements.

profiles. Again the temperature profiles increase monotonically with time, that is no relevant overshoots are observed in temperature, The same is true for run number 4, shown in Figs. 8 and 9. Here $U_{max}/U_\infty = 2.17$ in steady state, indicating that the forced flow is relatively stronger than in any of the previous runs. Agreement between the measured and computed temperature and velocity levels is generally good considering the uncertainties of the experiment.

SUMMARY AND CONCLUSIONS

An explicit finite-difference numerical technique was used to compute the transient aiding mixed convection flow, adjacent to a flat vertical surface. The surface was subjected to a sudden constant and uniform heat flux input. The temperature and velocity responses in the boundary layer were measured. Each experiment was repeated several times, with the probe positioned at different distances from the surface. Thereby instantaneous temperature and velocity profiles were measured at different times during the response.

Both measurements and calculations covered a range of input conditions. The surface input heat flux was varied from about 14 to 15 W m^{-2}, while the free-stream velocity was in the range 3–5.1 cm s^{-1}. Accordingly, the dimensional parameter $U_\infty = Re_x/(Gr_x^*)^{1/4}$ varied from 2.9 to 6.93. The relative magnitude of forced to natural convective effects is qualitatively assessed from the magnitude of U_∞. This is evident from the value of the ratio U_{max}/U_∞ as shown in Table 1. For large values of U_∞, forced convection effects are more prominent, and lead to a smaller value U_{max}/U_∞.

The measurements were generally found to be in good agreement with the numerical predictions, except during the early part of the transient. Then the measured response was more rapid than predicted by the computations. This is surmised to have arisen because the calculations were based on a heat flux value corrected for radiation at steady state. During the early transient however, radiation effects are considerably smaller than those at steady state. Another source of possible error in the measurements is the necessity to repeat each run several times, to measure the boundary-layer profiles. Since the runs were not exactly identical, the calculations were made for average values. The variation in input conditions among the different tests, however, was minimal, as shown in Table 1.

REFERENCES

1. E. M. Sparrow and J. L. Gregg, Buoyancy effects in forced convection flow and heat transfer, *Trans. Am. Soc. mech. Engrs*, Series E, *J. appl. Mech.* **26**, 133–134 (1959).
2. J. R. Lloyd and E. M. Sparrow, Combined forced and free convection flow on vertical surfaces, *Int. J. Heat Mass Transfer* **13**, 434–438 (1970).
3. P. H. Oosthuizen and R. Hart, A numerical study of laminar combined convective flow over flat plates, Report 4/71, Thermal and Fluid Sciences Group, Queen's University, Kingston, Ontario, Canada (1971).
4. J. Gryzagoridus, Combined free and forced convection from an isothermal vertical plate, *Int. J. Heat Mass Transfer* **18**, 911–916 (1975).

5. M. J. Hommel, Mixed convection heat transfer from a vertical plate: Prandtl number effects, ASME Winter Annual Meeting, New York (1976).
6. J. H. Merkin, The effect of buoyancy forces on the boundary layer flow over a semi-finite vertical flat plate in a uniform free stream, *J. Fluid Mech.* **35**, 439–450 (1969).
7. G. Wilks, The flow of a uniform stream over a semi-infinite vertical flat plate with uniform surface heat flux, *Int. J. Heat Mass Transfer* **17**, 743–753 (1974).
8. V. P. Carey and B. Gebhart, Transport at a large downstream distance in mixed convection flow adjacent to a vertical uniform flux surface, *Int. J. Heat Mass Transfer* **25**, 255–266 (1982).
9. R. Hunt and G. Wilks, Mixed convection—a comparison between experiment and an exact numerical solution of the boundary layer equations, *Letters Heat Mass Transfer* **9**, 291 (1982).
10. B. Sammakia, B. Gebhart and V. P. Carey, Transient mixed convection adjacent to a vertical flat surface, *Int. J. Heat Mass Transfer* **25**, 835–845 (1982).
11. R. P. Mahajan, Higher order effects, stability and transition in vertical natural convection flows. Ph.D. dissertation, Cornell University (1977).
12. V. P. Carey, Transport in vertical mixed convection flows and natural convection flows in cold water. Ph.D. dissertation, State University of New York at Buffalo (1981).
13. B. Sammakia and B. Gebhart, Transient and steady state numerical solutions in natural convection, *Numer. Heat Transfer* **1**, 529–542 (1978).

MESURES ET CALCULS DE LA CONVECTION MIXTE DANS L'AIR

Résumé—On présente des mesures et des calculs de convection mixte variable, adjacente à une surface plane et verticale. La surface dissipe un flux de chaleur constant et uniforme dans un écoulement d'air à vitesse ambiante constante et uniforme. La vitesse d'écoulement libre est dans la même direction que l'écoulement induit par gravité et il en résulte une convection mixte "aidée". Les mesures de température et de vitesse dans la couche limite sont présentées et comparées aux résultats d'une analyse par différences finies. Plusieurs niveaux de flux thermique et de vitesse forcée ambiante sont considérés.

MESSUNGEN UND BERECHNUNGEN DER TRANSIENTEN MISCHKONVEKTION IN LUFT

Zusammenfassung—Es werden Messungen und Berechnungen transienter Mischkonvektionsströmungen an einer flachen, vertikalen Oberfläche vorgestellt. Von der Oberfläche wird eine konstante und gleichförmig verteilte Wärmestromdichte an einen Luftstrom abgegeben, der mit einheitlicher und konstanter Umgebungsgeschwindigkeit strömt. Der freie Luftstrom und die durch den Auftrieb hervorgerufene Strömung sind gleichgerichtet. Temperatur- und Geschwindigkeitsmessungen in der Grenzschicht werden dargelegt und mit den durch ein Finite-Differenzen-Verfahren ermittelten Ergebnissen verglichen. Es werden unterschiedliche Wärmestromdichten und Umgebungsluftgeschwindigkeiten untersucht.

ИЗМЕРЕНИЯ И РАСЧЕТЫ НЕСТАЦИОНАРНОЙ СМЕШАННОЙ КОНВЕКЦИИ В ВОЗДУХЕ

Аннотация—Представлены измерения и расчеты нестационарных течений при смешанной конвекции у плоской вертикальной поверхности. Поверхность нагревается постоянным и однородным тепловым потоком и омывается струей воздуха, движущегося с однородной и постоянной скоростью. Скорость свободного потока имеет то же направление, что и вызванный нагревом поток, в результате которого возникает подъемное смешанно-конвективное течение. Представленные измерения температуры и скорости в пограничном слое сравниваются с данными, полученными в результате конечно-разностного анализа течения. Исследование проведено при различных величинах теплового потока и скоростей струи.